3-Dimensional Isotropic DWMRI in a Single Radial-FSE Scan

J. Sarlls[1], R. Newbould[2], S. Moore[1], M. Altbach[3], A. Gmitro[3,4], T. Trouard[1,3]

[1]Biomedical Engineering, University of Arizona, Tucson, Arizona, United States, [2]Radiology, Stanford, Stanford, California, United States, [3]Radiology, University of Arizona, Tucson, Arizona, United States, [4]Optical Sciences, University of Arizona, Tucson, Arizona, United States

Introduction

Radial-FSE methods have been used to produce high-resolution diffusion-weighted images that are insensitive to motion and/or magnetic field inhomogeneity. A unique feature of radial MRI is that the center of Fourier space is sampled with each line of data. When the radial lines have different weightings, e.g. T2 or diffusion, the resulting image will contain some combination of the weightings. In previous work, the diffusion and T2 weightings were controlled to obtain effectively isotropic diffusion weighting in a 2D radial-FSE sequence [1]. The extension of these ideas to 3-dimensional (3D) radial is presented herein. The ability to carry out radial 3D diffusion-weighted imaging allows high spatial resolution to be obtained in 3 dimensions while maintaining good SNR. In addition, 3D imaging allows the visualization of any plane of section in the DWMRI dataset, which could be very beneficial in diagnosis and evaluation of a number of neuropathologies. By obtaining effectively isotropic weighting in a single scan, total imaging time is minimized.

Methods

The 3D isotropic diffusion-weighted radial-FSE sequence contains a dual spin-echo preparation period during which diffusion gradients are applied. This preparation period is followed by a FSE acquisition train during which multiple radial lines of Fourier data (views) are collected. The number of views, their angular orientation and the order in which they are collected is completely flexible and has been shown to be critical to image quality in 2D radial-FSE MRI [2]. For picking the view orientations, points along a calculated spiral on the surface of a sphere were chosen such that the angular spacing in θ and ϕ are equal. For the examples shown in all figures, 4096 views were collected with an etl = 8. The direction of diffusion weighting is altered during the scan four times using [1,1,1], [-1,1,1], [1,-1,1], and [-1,-1,1] (indicating full gradient strength on the [X,Y,Z] axis) to attain isotropic diffusion weighting when averaged [1]. Two different view ordering schemes were implemented. The first is a simple sequential view order where each view is collected sequentially in time, beginning with the view oriented at ϕ = 0° and spiraling around in θ, down to ϕ = 90°. The second ordering was designed to mimic the attributes of the bit-rev view ordering from the 2D technique [1]. It was chosen to coarsely sample the full volume of k-space within each TR period, and to generate a high frequency angular variation in both TE and diffusion direction for adjacent views, without correlation of diffusion weighting direction with particular TE values.

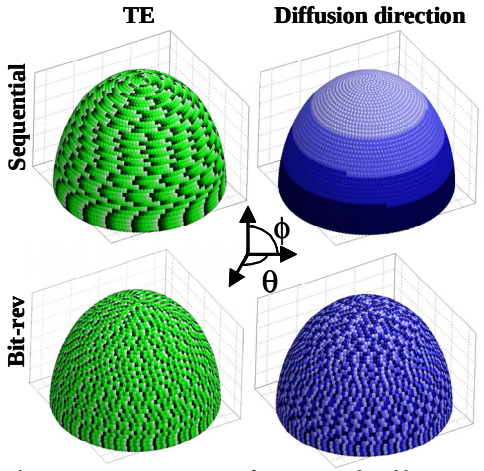

Fig. 1. View starting points for sequential and bit-rev view ordering schemes are shown. In the plots for TE, the lightest green color represents TE1 and the darkest TE8. Each of the four diffusion directions are plotted in a different shade of blue.

Results

The angular variation of TE and diffusion weighting direction for the sequential and bit-rev view ordering schemes are shown in **Fig. 1**. There is an obvious low frequency angular variation of both TE and diffusion weighting using the sequential ordering, while the bit-rev ordering has more high frequency variation in both. Images obtained using the sequential or bit-rev view ordering are shown in **Fig. 2**. For the non-diffusion-weighted images, **Fig. 2a** and **c**, there is little artifact due to T2 decay in either dataset. This is in contrast to 2D radial-FSE imaging where significant streaking is observed with sequential ordering [2]. The difference is likely due to the variation of TE in the ϕ direction for the 3D imaging. Conversely, using sequential view ordering in diffusion direction causes more significant problems, as seen in **Fig. 2b**. In regions of high anisotropy, e.g. the corpus callosum, there is considerable brightness and streaking due to tissue anisotropy with sequential ordering. Using the bit-rev view ordering, these same structures are isointense and do not have artifactual signal variation (**Fig. 2d**). This is also true of the images in **Fig. 3**, taken from a 3D dataset of a stroke patient collected using the bit-rev view order. A small ischemic lesion (arrows) is seen as an area of hyperintensity in the two orientations. Multiple planes of section allow the full extent of the stroke to be visualized.

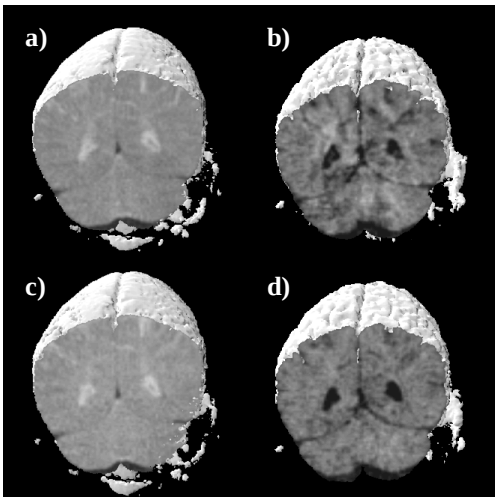

Fig. 2. Parameters for all images: TE=87 ms, TR=500 ms, ETL=8, FOV=22 cm, 1.7mm^3 isotropic voxels, acquired on 1.5T scanner. In **a)** and **b)** data acquired with sequential view ordering; **c)** and **d)** data acquired with bit-rev view ordering. **a)** and **c)** b = 0 s/mm^2; **b)** and **d)** b=1000 s/mm^2 with isotropic diffusion weighting.

Conclusion

Radial-FSE methods allow high-resolution 3D diffusion-weighted MRI to be carried out with little artifact due to motion and/or magnetic field inhomogeneity. By using appropriate view ordering and diffusion weighting schemes, effectively isotropic diffusion weighting can be obtained in a single 3D radial-FSE exam with minimal artifacts due to both T2 decay and diffusion anisotropy. The ability to visualize lesions with high-resolution in any plane will allow more accurate measurements of lesion volume.

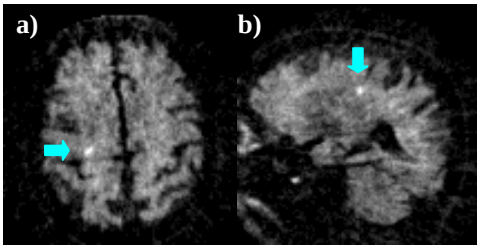

Fig. 3. Two orthogonal slices of a stroke patient from an isotropic diffusion-weighted 3D radial-FSE dataset. Imaging parameters: TE=87 ms, TR=500 ms, ETL=8, FOV=22 cm, bit-rev view order, b=1000 s/mm^2, 1.7mm^3 isotropic voxels, acquired on 1.5T scanner. **a)** conventional axial slice showing an hyperintense area of ischemic tissue (arrow), **b)** same area of ischemia viewed in a sagital slice (arrow).

References: [1] Sarlls, *et al*., *M.R.M*., in press. [2] Theilmann, *et al*., *M.R.M*., 51, 768-774, 2004.

Acknowledgements: This work supported by NIH grant R21 AG021624.